Cell Based Modeling of Arteriosclerosis

by
Megan Knapp

Abstract

Studying how mesenchymal cells organize to cause arteriosclerosis, a disease where the mesenchymal cells on the vascular wall of the arteries or the cardiac valves turn to bone tissue and harden, could give insight into its cellular mechanisms. Mesenchymal cells secrete the morphogen activator bone morphogenic protein (BMP-2) and the inhibitor matrix carboxyglutamaic acid protein (MGP) that drive the formation of striped patterns. Previous continuum models (Garfinkel et al. [3]) can predict this pattern formation by displaying high concentrations of BMP-2. This model uses the reaction-diffusion equations to adjust the concentrations of the morphogens over time by having them fuel their own production autocatalytically. However, the Garfinkel et al. model omits the cells and assumes cellular signals even in the absence of cells, thus neglecting the cells' feedback. In order to make the model closer to how a biological system actually works a cell based model is needed. Our cellular Potts model substitutes autocatalytic production of BMP-2 for chemotactic recruitment of mesenchymal cells.

A thesis submitted to the Department of Physics and Astronomy in partial fulfillment of requirements for a bachelor's degree. Supervised by Stephen Teitel (University of Rochester) and Roeland Merks (Indiana University)

University of Rochester
Rochester, New York
2005

1 Introduction

1.1 Arteriosclerosis

Unspecialized mesenchymal cells differentiate or morph into a variety of connective tissues such as fat, bone tissue and cartilaginous tissue[1]. In adult diseases like arteriosclerosis, these cells differentiate into many different types of cells like osteoblasts (bone cells) and aggregate within the artery wall resulting in vessel hardening[2]. Arteriosclerosis occurs in the aorta and on artery walls where the mesenchymal cells on the inside of the vascular wall calcify into bone tissue. The bone tissue forms focal and nodular patterns, a process occurring throughout the blood vessels in atherosclerotic lesions [3].

Mesenchymal cell tissue cultures provide a popular *in vitro* model of arteriosclerosis. When mesenchymal cells are placed in a tissue culture they sort to form a striped pattern [3]. Fig. 1 shows the development of the cell aggregation over 20 days. The cells develop from swirls to stripes, eventually calcifying into the bone mineral hydroxylapatite [3]. Garfinkel et al. observe that the cells "can be seen to orient perpendicular to the edges of the multicellular ridge" [3] and conclude that the mesenchymal cells aggregate into striped patterns as a result of a process known as chemotactic migration.

Chemotaxis is a mechanism whereby a chemical guides cell aggregation [5]. Cells migrate up gradients of a chemical called a chemoattractant. Such chemotactic migration, or chemotaxis, occurs in many different types of cells, such as in nerve cells and endothelial cells which line the blood vessel walls. Aggregation plays a role in several biological systems, like in *Dictyostelium discoideum* where chemotaxis causes all the cells to move together to form something similar to a "slug"[8]. When a certain type of cell is in the presence of its chemoattractant, it moves up the concentration gradient toward the highest concentrations of the substance. During processes such as embryonic development, one cell type will secrete a chemoattractant for a different cell type[10]. Oftentimes, as is the case with mesenchymal cells, the cell will secrete its own chemoattractant, making cells clump.

Mesenchymal cells secrete bone morphogenic protein (BMP-2) and matrix carboxyglutamaic acid protein (MGP) [3][1]. BMP-2 is a chemoattractant [3]. MGP serves as an inhibitor for BMP-2 by decreasing part of the BMP-2 signalling system and increasing its binding to the extracellular matrix, a protein web that provides the scaffolding that keep the cells in position[7]. This binding has the effect of decreasing the cells' ability to move around,

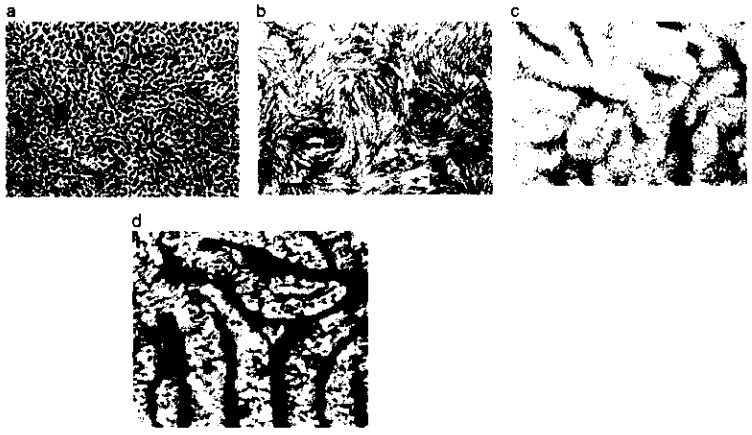

Figure 1: From Garfinkel et al.[3] Vascular mesenchymal cells (VMCs) aggregating *in vitro* over a 20 day period. (a) The initial random assortment of VMCs (approximately day 1) (b) swirl patterns form (approximately day 4), (c) the cells form stripe-like patterns(approximately day 10), (d) the final labrynthine pattern (approximately day 16). [Bar= 250μm (a and b); c and d are at the same magnification as b]

because they are being held stationary in the protein web of the extracellular matrix. MGP diffuses more rapidly than its activator because of its smaller molecular mass [4]. Because of the properties of these two chemicals, Garfinkel et al. suggest that these are the chemicals that play the major role in the pattern formation of vascular mesenchymal cells [3].

1.2 Reaction-Diffusion Models

In 1952, Turing created a new approach to explain possible mechanisms of idealized embryo development using reaction-diffusion equations, explaining how periodic patterns emerge from a homogeneous field of chemicals. In his paper [6], Turing describes how the interaction of chemical substances called morphogens diffusing through a system of cells can account for most morphogenesis, the development of an organism from an embryo. A morphogen controls the growth patterns of tissues, which is very important in embryonic development [6]. All that is necessary in Turing's model is a minimum of two morphogens, the first enhancing cell growth and the other inhibiting it. As

the chemicals diffuse throughout a ring of cells, "chemical waves" are produced. The initially homogeneous stable state of the ring of cells is disturbed slightly by an internal or external process. Slow changes to the arrangement of the cells form patterns because of the cells' response to the morphogens. Small instabilities in the configuration of cells may effect the immediate area surrounding the cell but have no effect far away because the morphogens only diffuse over a finite area[6]. Over the years, this method has been modified and used to model a variety of different chemical and biological systems [3]. Turing-like models, involving activator and inhibitors, have been studied for a long time. An activator is a morphogen that acts over a short range. An inhibitor acts over a longer range and diffuses faster than the activator. As happens in the vascular mesenchymal cell reaction-diffusion model described below, activator-inhibitor models use auto- or cross catalysis to account for pattern formation from graded distributions of the morphogens. The chemical gradients are controlled by the morphogens' diffusion and decay within the system of cells [11].

Garfinkel et al. use the reaction-diffusion equations to model the interaction of BMP-2 (U) and MGP (V) in mesenchymal cells. Their equations are:

$$\frac{\partial U}{\partial t} = D(\nabla^2 U) + \gamma \left[\frac{U^2}{(1 + kU^2)V} - cU \right] \tag{1}$$

$$\frac{\partial V}{\partial t} = (\nabla^2 V) + \gamma [U^2 - eV + S] \tag{2}$$

where $U(x, y)$ and $V(x, y)$ are the effective concentrations of the activator and inhibitor respectively at position (x, y). In these equations, the diffusion term where $D = D_U/D_V$ is the ratio of the diffusion coefficients.

Autocatalysis is the process by which the presence of one substance causes more of the same substance to be produced in that area. The most interesting term in Eq. (1) is the autocatalytic term with the U^2. So that the morphogen is not produced indefinitely, Eq. (1) has a saturation component of $1/(1 + kU^2)$. The inhibitor reduces the concentration of the activator by reducing BMP-2 production in areas of high MGP concentration. This relationship is incorporated into Eq. (1) by the $1/V$ component of the autocatalytic term. The production of MGP in Eq. (2) depends heavily on the concentration of BMP-2. Both equations have a degradation term where c and e are the degradation rates of the activator and inhibitor respectively. For the inhibitor

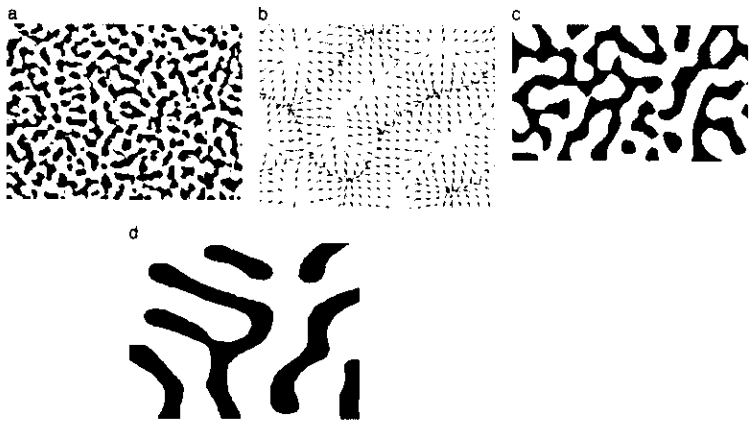

Figure 2: from Garfinkel et al.[3] Numerical solutions of Eqs. (1) and (2) corresponding to the same points in development as in Fig. 1. The black in the pictures are high levels of U, not cells. (a) Random spotty patterns of high concentrations of U form. (b) The arrows show that U increases in a specific direction, grad U, which would correspond with cell orientation in a cell culture had there been cells in the system. (c) Stripe-like concentrations of U develop. (d) The labrynthine pattern forms. The length scale of the simulation is the same as those in the cell culture

there is an exogenous or external source term, S, that describes the external addition of MGP in Garfinkel et al.'s experiments. One of the characteristics of the pattern formation predicted by the reaction-diffusion model is that by adding a constant amount of MGP to the system, the patterns change from stripes to spots[3]. The reaction-diffusion equations model concentrations of the chemicals, not of the cells themselves. Fig. 2 shows Garfinkel et al.'s simulated concentrations of the activator, represented in black, at different times.

In their *Supporting Text*, Garfinkel et al. add another equation to the reaction-diffusion Eqs. (1) and (2) in an attempt to take into account cell density, n [3],

$$\frac{\partial n}{\partial t} = \nabla \cdot \left(\nabla n - \frac{\chi_0}{(1+U^2)} n \nabla U \right). \tag{3}$$

Eq. (3) only allows the system to regulate the cells, but not for the cells to

feedback on the system. The activator and inhibitor determine the migration of the cells in Eq. (3), but the cell density n does not affect the concentration of the morphogens i.e., n does not enter any of the terms in Eqs. (1) and (2). Garfinkel et al. propose that adding cell density equations will not significantly change the pattern formation, but in their model the concentration of cells does not effect the concentration of the morphogens. It assumes cellular signaling even though the model does not have cells in it. The cells therefore do not give feedback to the morphogen concentrations. The only new thing Eq. (3) takes into account is cell migration up activator gradients [3]. In a real system, the cells secrete BMP-2 and MGP, so cell density is very important. The more cells concentrated in an area, the higher the concentration of the chemoattractant and the inhibitor will be. The autocatalytic term in the reaction-diffusion equations tries to account for this principle but in order to more closesly model a real system the cells should be secreting the morphogens. The goal of this thesis will be to construct such a model in order to account for the cells secreting the morphogens, as well as responding to the chemoattractant. We intend to replace the autocatalytic term by the more biologically realistic cell migration.

2 Methods

2.1 Cellular Potts Model

Continuum models, like the reaction-diffusion model, can efficiently model the extracellular matrix, fluids, and other noncellular materials like bone, but often are unable to reproduce tissue level processes originating from the collective behavior of cells[12]. Cell-centered models use biological experiments from the scientific literature as a basis for determining which cell behaviors to include and allow us to add more cell behaviors if the model does not reproduce experimental observations[12]. Once one pattern formation can accurately be reproduced, we can alter the parameters to predict new pattern formations that can then be verified experimentally [12]. The cellular Potts model accomodates many cellular behaviors by modeling the cell membrane and cell dynamics on a mesoscopic level [12]. This model is one method that has been developed to efficiently predict cell pattern formation. In the cellular Potts model, the cells explore different configurations in order to find the one with the lowest energy. Most cell behavior, such as cellular

adhesions and cellular responses to a chemical, can be represented as terms of a generalized energy called a Hamiltonian [12]. The model uses a Monte Carlo model which uses Metropolis dynamics to determine how cells move.

In the cellular Potts model the features of cells are represented by the sites of a discrete lattice. Each site on the lattice has a degree of fredom σ, which we will call a "spin". The value of σ denotes the presence of either an individual cell or the background host, the medium. The "spin" can take on one of the discrete values 0,1,2,...,N where 0 denotes the host medium and $\sigma = n$ denotes the presence of cell number n. Individual cells extend over multiple lattice sites and are represented by a connected cluster of sites with the same value of σ. Every cell has an area and a cell type associated with its spin σ. The area, $a(\sigma)$, is just the number of lattice sites covered by the individual cell. The cell type, $\tau(\sigma)$, determines a variety of characteristics associated with the particular cell. For example, these characteristics could include whether it secretes certain chemicals, adheres to different types of cells in a specific way, responds to chemical substances uniquely, and has a unique target area. This target area, $A_{\tau(\sigma)}$, is the cell type τ's ideal size. The adhesion of one cell to another, $J(\tau(\sigma), \tau(\sigma'))$, takes on different values depending on the type of cells, σ and σ', involved. In a system of multiple cell types, every different cell type has a specific strength of how well the cell binds to its own type, different types, and the medium. In our model of mesenchymal cells the only relevant adhesions are between the mesenchymal cells and between the mesenchymal cells and the medium. For a basic cellular Potts model, the area and the adhesion give the terms that form the Hamiltonian, the energy of the system [9]. If (i, j) denotes the coordinates of a site of the two dimensional lattice of points defining the model, then the Hamiltonian is given by:

$$\begin{aligned} H &= \sum_{(i,j)(i',j')neighbors} J(\tau(\sigma(i,j)), \tau(\sigma(i',j')))(1 - \delta_{\sigma(i,j),\sigma(i',j')}) \\ &+ \lambda \sum_{\sigma} (a(\sigma) - A_{\tau(\sigma)})^2. \end{aligned} \tag{4}$$

To implement the cellular Potts model, the simulation starts with a random configuration of cells over the lattice. Then it selects a random site and a random neighboring site tries to copy into the first site. The difference in the Hamiltonian ΔH from before the neighbor site tries to copy into the random site, and after it copies, is put into a probablility function [9] to

decide whether the copying will occur:

$$P(\sigma(i,j) \rightarrow \sigma'(i,j)) = \begin{cases} e^{(-\Delta H/k_B T)} & \text{if } \Delta H > 0 \\ 1 & \text{if } \Delta H \leq 0 \end{cases} \tag{5}$$

In Eq. (5), $k_B T$ is the Boltzman energy that accounts for thermal energy of the system. As usually happens in thermal systems, there is a threshold temperature above which the cells will not aggregate any more because it is too hot, and a critical temperature below which the cell movement freezes [9]. Once it is decided whether the site will copy or not according to the probability of Eq. (5), another site is chosen at random and the process repeats.

2.2 Cellular Potts Model for Modelling Vascular Mesenchymal Cells

In order to adapt the reaction-diffusion model to the the cellular Potts model, Eqs. (1) and (2) have to be modified to include cellular feedback. Using the Potts model, we aim to drop the biologically non-realistic autocatalytic term and have the cells secrete BMP-2 and MGP themselves. As cells aggregate, the concentration of both the activator and inhibitor should increase since the cells are secreting them at a more or less constant rate. In the model, the morphogens only degrade outside of the cells. Adapting the reaction-diffusion equations to include the cellular Potts model, the equations become:

$$\frac{\partial U(i,j,t)}{\partial t} = D(\nabla^2 U) + \gamma_u [\frac{1 - \delta_{\sigma_{(i,j)},0}}{(1 + kV(i,j,t))} - cU(\delta_{\sigma_{(i,j)},0})] \tag{6}$$

$$\frac{\partial V(i,j,t)}{\partial t} = (\nabla^2 V) + \gamma_v [(1 - \delta_{\sigma_{(i,j)},0}) + \delta_{\sigma_{(i,j)},0}(eV - S)]. \tag{7}$$

Here k is a scaling term that regulates the degree to which the inhibitor gives feedback to the system. The reaction-diffusion equations have been discretized to the same grid of sites as used in the cellular Potts model. $U(i,j,t)$ and $V(i,j,t)$ are the chemical concentrations on the site (i,j) at time t. The Kronecker delta in these equations separates the processes that happen inside the cell from those that happen outside. For example, $\delta_{\sigma(i,j),0}$ will be 1 if $\sigma(i,j) = 0$ meaning the degradation happens outside of the cells.

Other parts of the Potts model remain basically the same as the standard model. The general equation for the Hamiltonian in the original model still

holds, but needs to have an additional term to take into account the energy lost to chemotaxis. Because the cells are moving up BMP-2 gradients, energy will be transferred in the system. The Hamiltonian of the system becomes:

$$H = \sum_{(i,j)(i',j')neighbors} J(\tau(\sigma(i,j)),\tau(\sigma(i',j')))(1-\delta_{\sigma(i,j),\sigma(i',j')}) \quad (8)$$

$$+ \lambda \sum_{spins\ \sigma} (a(\sigma)-A_{\tau(\sigma)})^2 - \sum_{i,j} \chi \frac{U(i,j,t)}{sU(i,j,t)+1}(1-\delta_{\sigma(i,j),0}) \quad (9)$$

In Eq. (9), χ is the strength of the chemoattractant response. The parameter s is the Michaelis-Menten constant of chemotactic response that controls how well the cell reacts to the chemoattractant[5].

The first step in the algorithm is to run a full Monte Carlo step of selecting random sites on the lattice, $\sigma(i,j)$, compute the Hamiltonian and update the cell pattern for each random site. Then the next step is to run though every site on the lattice and alternate between secreting or degrading the chemicals and diffusing the morphogens twenty times to ensure the chemicals have increased and diffused sufficiently over the entire lattice. Because of the time it takes for the chemicals to be produced and then diffuse over the lattice, each round of secretion, degradation, and diffusion corresponds to a certain period of time characteristic of the chemicals involved. For any lattice site that corresponds to a cell, the algorithm updates the chemical concentrations according to:

$$U(i,j,t+dt) = U(i,j,t) + \frac{dt\gamma_u}{1+kV(i,j,t)} \quad (10)$$

$$V(i,j,t+dt) = V(i,j,t) + dt\gamma_v \quad (11)$$

where dt is a constant representing the time increase. Whenever the site is outside a cell, the chemical concentrations update according to a different set of equations:

$$U(i,j,t+dt) = U(i,j,t) - dt\gamma_u cU(i,j,t) \quad (12)$$

$$V(i,j,t+dt) = V(i,j,t) - dt\gamma_v[eV(i,j,t) - S]. \quad (13)$$

In the last step of the process, both chemicals are then diffused over the entire lattice, regardless of whether any site is inside or outside a cell. The

boundaries of the lattice are no flux so the cells do not adhere to the edges of the simulation space. The ∇^2 terms in Eqs. (6) and (7) are taken as the discrete Laplacian defined by

$$\nabla^2 U(i,j) = U(i+1,j)+U(i-1,j)+U(i,j+1)+U(i,j-1)-4U(i,j) \quad (14)$$

$$\nabla^2 V(i,j) = V(i+1,j)+V(i-1,j)+V(i,j+1)+V(i,j-1)-4V(i,j). \quad (15)$$

When diffusion occurs, the concentration of the chemicals at every site is then replaced by the equations:

$$U(i,j,t+dt) = U(i,j,t) + \nabla^2 U(i,j,t)dtD \quad (16)$$

$$V(i,j,t+dt) = V(i,j,t) + \nabla^2 V(i,j,t)dt \quad (17)$$

Once the diffusion has been evaluted, a new timestep begins and the process repeats.

2.3 Methods of Analysis

Once the simulation runs for a specified number of Monte Carlo steps, the lattice of cells and chemical concentrations is converted to an image. The lattice points corresponding to the medium (where $\sigma(i,j) = 0$) become white, while the lattice points corresponding to cells (where $\sigma(i,j) \neq 0$) become red. Any place where there are two different values of $\sigma(i,j)$ next to each other, a black cell boundary is produced. Finally, the chemical concentrations are converted to contour lines of equal concentration. The activator morphogen $U(i,j)$ is green and the inhibitor morphogen $V(i,j)$ is purple. An example of such an image resulting from our simulation is shown in Fig. 3. The image produced from the lattice then needs to be analyzed to quantify the nature of the cell pattern formation.

An important goal of running these simulations is to ensure that the labrynthine patterns formed by the simulations are not becoming larger indefinitely, but that instead the width of the white space approaches a characteristic wavelength. We use the method of autocorrelations to determine whether the width of the stripes is finite.

In this method, the image is converted into a matrix $B(i,j)$ where $B(i,j) = 1$ if a cell occupies the site (i,j) and $B(i,j) = 0$ otherwise. The Wiener-Khinchin Theorem is then used to quickly calculate the autocorrelation func-

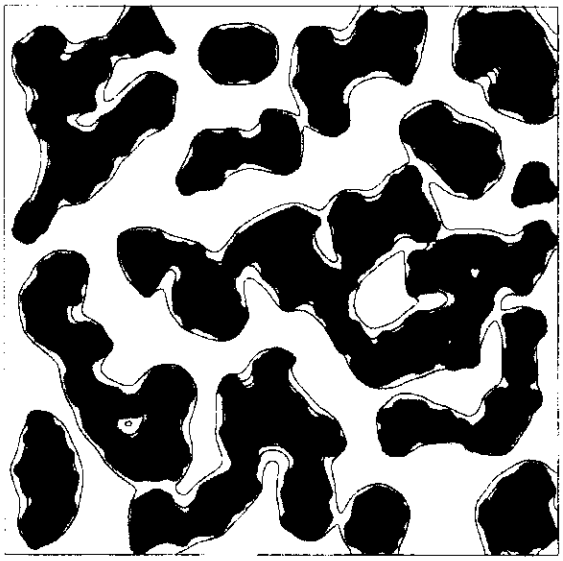

Figure 3: An example of the result of a simulation. Lattice size is 400×400.

tion in Fourier space. First, the discrete Fourier transform of the matrix is found using the equation:

$$\tilde{B}(\vec{k}) = \sum_{\vec{r}} B(\vec{r}) e^{i\vec{k}\cdot\vec{r}}. \tag{18}$$

In the vector $\vec{r} = (i, j)$, both i and j run from 0 to $L - 1$, where L is the length of the simulation lattice. $B(\vec{r})$, then, is the value (1 or 0) of the matrix at the site $\vec{r} = (i, j)$. The autocorrelations, A, of the image are then given by:

$$A(\vec{r}) = \sum_{\vec{k}} [e^{-i\vec{k}\cdot\vec{r}} \left| \tilde{B}(\vec{k}) \right|^2]. \tag{19}$$

The vector $\vec{k} = (k_x, k_y)$, with $k_x = \frac{2\pi}{L} n_x$ and $k_y = \frac{2\pi}{L} n_y$, and the variables $n_x, n_y = 0, 1, \ldots, L - 1$. The vector $\vec{r}$ is recentered so that $i, j = -\frac{L}{2}, \ldots, \frac{L}{2}$. Then we sum up all the contributions to a certain direction using angular integration of $A(\vec{r})$ to get the autocorrelation, $C(r)$, as a function of the distance between two points independent of the orientation of the line connecting those points. The angular integration is:

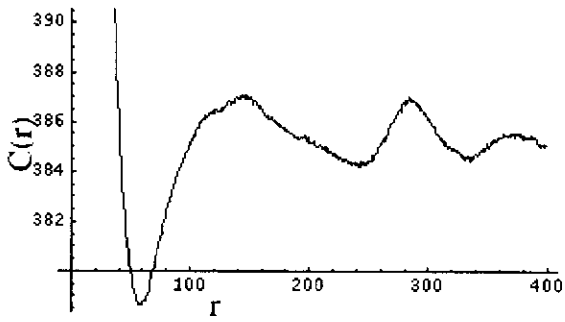

Figure 4: Plot of the autocorrelations. The absolute minimum represents the thickness of the stripes and the first maximum represents the width of the gaps. The initial number of cells was 1350. There was no source term. The correlation was computed after 84000 MCS.

$$C(r) = \frac{1}{2\pi} \int_0^{2\pi} A(r\cos\phi, r\sin\phi)\, d\phi. \tag{20}$$

Eq. (20) is evaluated by approximating

$$\phi_i = \frac{2\pi}{N} i \tag{21}$$

$$x_i = int[(r + \frac{1}{2})\cos\phi_i] \tag{22}$$

$$y_i = int[(r + \frac{1}{2})\sin\phi_i] \tag{23}$$

where $N = 100$ and $i = 0, \ldots, 99$. The terms x_i and y_i are taken to be integers to ensure that they refer to points of $A(\vec{r})$. The autocorrelation, $C(r)$, is then approximated by:

$$C(r) \simeq \frac{1}{N} \sum_{i=1}^{N} A(x_i, y_i) \tag{24}$$

An example of the autocorrelation is shown in Fig. 4. The value of r at the absolute minimum of $C(r)$ represents the thickness of the stripes. The value of r at the first maximum value represents the width of the gaps. If over time this width approaches a constant value, then the distance between the stripes is not growing indefinitely, and the pattern formed is stable.

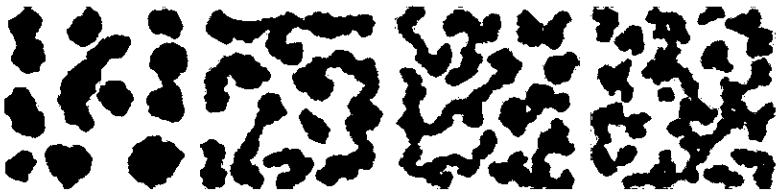

Figure 5: Increasing values of the parameter k at 20000 MCS. $k = 2, 4, 6, 8$ respectively. The parameter $\gamma = .5$.

3 Results

3.1 Parameters

The parameters in the Hamiltonian stayed largely fixed once a value that corresponded to the physical parameters and which produced the striped patterns was found. In these simulations, the dimensionless scaled value of the temperature, T, in Eq. (5) is 10, which corresponds to the usual temperature of the cell cultures at $37°C$. We chose the dimensionless energy of $J_{cell-medium}$ to be the same as the dimensionless temperature as a way of scaling all the energies in the Hamiltonian. In the units of our simulation, 10 is room temperature. The cell-cell adhesion value, $J_{cell-cell} = 20$ and the cell-medium adhesion value, $J_{cell-medium} = 10$, were set to ensure the cells adhered to each other twice as much as they adhered to the medium. While this choice of values allows the cells to favor binding to each other rather than to the medium; it still allows the cells freedom to move around. The parameter χ from Eq. (9) is the strength of chemotactic response, making the constant specific to the cellular Potts model. Its value was determined by studying the rate of pattern formation by cells for different values of χ. If the parameter is much larger than 5, the cells stay in one place longer because it is hard for them to move. Similarly, if χ is too small the cells move too easily. The value of $\chi = 5$ is a good balance between these extremes.

Although it is not a parameter per se, the spatial dimension in the cellular Potts model simulation differs from the length of the cell culture and Garfinkel et al.'s simulation. While the cell culture and Garfinkel et al.'s simulation lengths were 4 cm across, ours was only 1 mm. The number of computations required by a larger lattice makes the simulation prohibitively long.

The parameters in the equations regulating the concentrations of the morphogens contribute more to the pattern formation. As evidenced by Fig. 5, we chose $k = 6$ in Eq. (6) because at that value the cells form stripes. The parameter k controls the effect of the inhibitor on the production of BMP-2.

As in Garfinkel et al., D is the ratio of the diffusion coefficients. The diffusivity of BMP-2 and MGP have not been directly measured in experiments, but since these molecules are similar to other molecules whose diffusivity has been determined, it is possible to approximate the diffusivity of these morphogens [4]. To estimate the diffusion coefficient of the BMP-2, we compared this activator to a protein, decapentaplegic, that has similar structure and diffusion behavior and diffuses at a rate of $\approx .1 \times 10^{-8} cm^2/sec$ [4]. Because the diffusion of large molecules slows nonlinearly due to of the extracellular matrix, their diffusivity can be reduced as much as 10 to 20 fold in muscle tissue [4]. Keeping this in mind, the diffusion of BMP-2 was estimated as $0.3 \times 10^{-8} cm^2/sec$. The diffusivity of MGP was kept as the same estimated value as Garfinkel et al., $30 \times 10^{-8} cm^2/sec$. Using these estimated diffusion coefficients, $D = D_U/D_V \approx 1/100$.

To estimate the degradation rates of the morphogens, the same protein that was used to estimate the diffusion rate of BMP-2, decapentaplegic, was examined. It was found to be 5% of the production rate [4]. Therefore, conservatively estimating the degradation of BMP-2 to be 0.5% of the production rate ($c = .005$) is reasonable. Garfinkel et al. found that the extracellular matrix takes up MGP more avidly than BMP-2, therefore estimating the degradation of MGP to be 5% of the production rate ($e = .05$) is a reasonable estimate.

The values of the parameters used in our simularion are summarized in table 1.

3.2 Cell Aggregation

Fig. 1 shows experimentally obtained striped patterns of mesenchymal cells as time evolves. The cellular Potts model also predicts the striped formations. Fig. 6 shows the labrynthine patterns. The stripes do not have as many "Y-connections" (they are not as interconnected) as the cell cultures in Fig. 1 do. There are also more clusters of cells that are not connected to a stripe. This is not changed by running the simulations for more Monte Carlo steps. The only effect a longer simulation time has is that the stripes become slightly more connected and any "holes" in the clumps of cells disappear. Adding more

Table 1:

Parameter	Estimated Physical Value	Cellular Potts Value	Reaction Diffusion Value
χ		5	
Adhesion			
$J_{cell-cell}$	—	20	—
$J_{cell-medium}$		10	—
Temperature			
T	$37°C$	10	–
Length of			
L	4 cm	1 mm	4 cm
Diffusion Coefficients			
D_u in cm^2/sec	$\approx .1 \times 10^{-8}$	$.3 \times 10^{-8}$	$.15 \times 10^{-8}$
D_v in cm^2/sec	$\approx 30 \times 10^{-8}$	30×10^{-8}	30×10^{-8}
D	—	1/100	1/200
Degradation Rates			
BMP-2 (c)	5%	.5% ($c = .005$)	1% ($c = .01$)
MGP(e)	$\approx 10\%$	5% ($e = .05$)	2% ($e = .02$)
γ_u	—	.1-.9	—
γ_v	—	.1-.9	—
Source term S	40ng/ml	.003-3	6×concentration

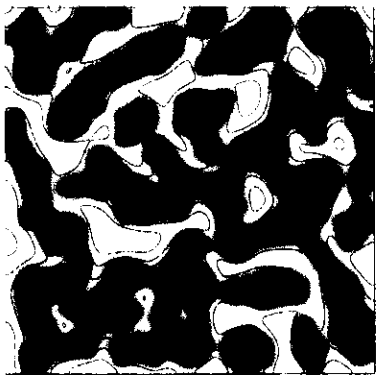

Figure 6: After 40000 MCs, the pattern forms stripes that do not have many "Y-connections". Initially, there are 1350 cells in this simulation.

Figure 7: After 40000 MCS, the pattern is more connected and striped. There are initially 1800 cells in this simulation instead of 1350. The source term S=.6.

cells to the simulations initially makes the patterns become more connected, and form more of a striped pattern as in Fig. 7.

The cellular patterns evolve over the Monte Carlo steps, just as a cell culture develops over time. As shown in Fig. 8, the patterns develop from a random assortment of cells into swirls and finally into stripes similar to the cell culture in Fig. 1. Looking at how the pattern develops over time and comparing it to how patterns evolve in cell cultures, each Monte Carlo step can be determined to correspond to about 10 min/MCS in real time. Autocorrelations on pictures over several different Monte Carlo steps show that the width between the stripes approaches a constant value. As shown in Fig. 9, after about 50000 MCS the width of the stripes does not grow anymore. However by about 20000 MCS the pattern is formed well enough that the additional tens of thousands of Monte Carlo steps does not make a significant difference.

Any variations in the parameters γ_u and γ_v alters the pattern. These parameters appear in Eqs. (6) and (7) as means of scaling the extent of productino and degradaton of the corresponding morphogen. Fig. 10 shows that as the parameter γ_v (which scales the production rate of MGP) increases, the stripes become finer. According to Garfinkel et al., more MGP in the system causes the chemoattractant to have its strongest concentration close to the cell patterns, forming spots. In cellular Potts simulations, the concentration gradients of MGP show that when $\gamma_v = .9$ and $\gamma_u = .1$ the MGP gradients

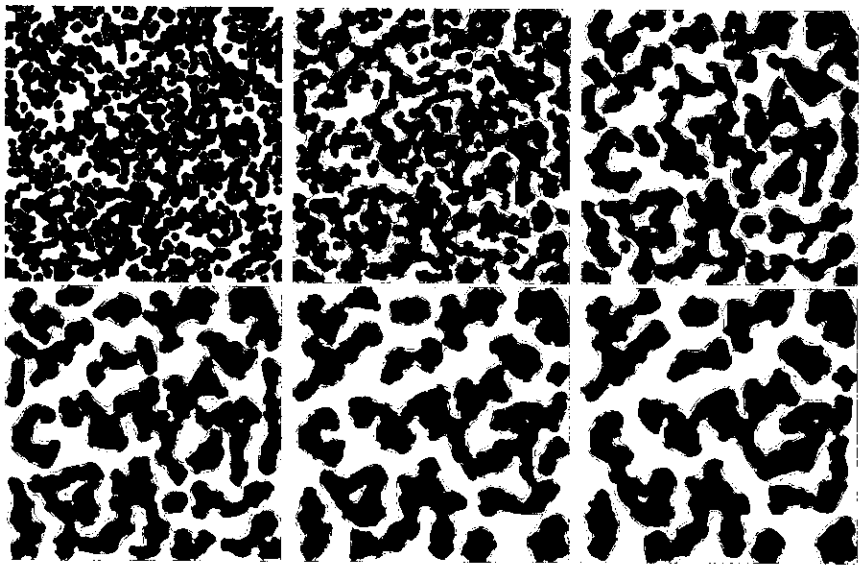

Figure 8: Increasing MCS. MCS: 0,500,1500,3000, 7000, and 10000. There are initially 1350 cells in this simulation.

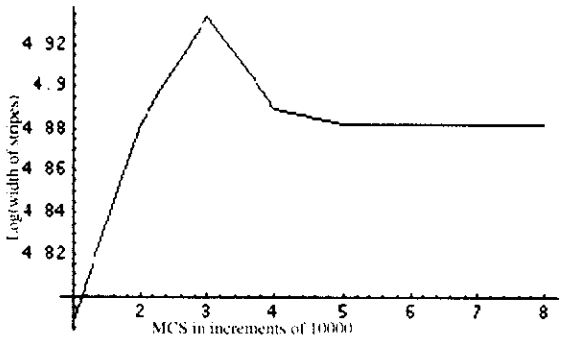

Figure 9: Logarithm of the width of the stripes over time. Each new picture was after 10000 MCS beginning at 10000 MCS. The source term S=.06, 1350 = initial number of cells

are just as steep and close to the cell as the BMP-2 gradients, so the cell patterns are being sculpted into fine patterns.

The parameter γ_u scales the production of BMP-2. Garfinkel et al. found that in cell cultures as more BMP-2 was present in the system, the stripes became thinner, causing a finer labrynthine pattern. In the cellular Potts simulations of Fig. 10, the stripes thicken and almost become spot-like as γ_u increases. This result is opposite from Garfinkel et al.'s result. When $\gamma_u = .9$ and $\gamma_v = .1$, the BMP-2 gradients are steeper and closer to the cells that they are when $\gamma_u = .1$. This means that the BMP-2 is acting closer to cell clumps keeping the cells from spreading out at the higher production rates.

Adding an exogenous (outside) source of MGP to the cells caused spots to form instead of stripes in cell cultures [3]. However, adding a source term of MGP in the cellular Potts model does not have this same effect. In Fig. 11, we see that the cells form stripes, regardless of how much MGP is added to the system, until finally the cells dissociate into a random configuration. The concentration gradients of MGP spread out because there is much more of the morphogen to diffuse over the entire system while the concentration gradients of BMP-2 are steep and stay close to the cell since it is not highly concentrated enough to move far from its production site. This is because the source term, S in Eq. (7) increases the concentration of the inhibitor so much that the chemoattractant is produced at a low rate. Therefore there is not enough of the chemoattractant to cause the cells to form large clumps. Adding too much inhibitor causes the cells to dissociate into a random assortment because the chemoattractant never has a concentration high enough to have an effect on the pattern. Changing the production rates of the inhibitor and chemoattractant while still adding an exogenous source of MGP does make the pattern form something other than stripes as shown in Fig. 12. In this figure, the concentration of the chemoattractant remains close to the cells while the inhibitor spreads out. Running the simulation for more Monte Carlo steps with the original number of cells produces fully formed spots under the inlfuence of the γ parameters as shown in Fig. 13. So the cellular Potts model does produce spots, just not by a process that was originally expected.

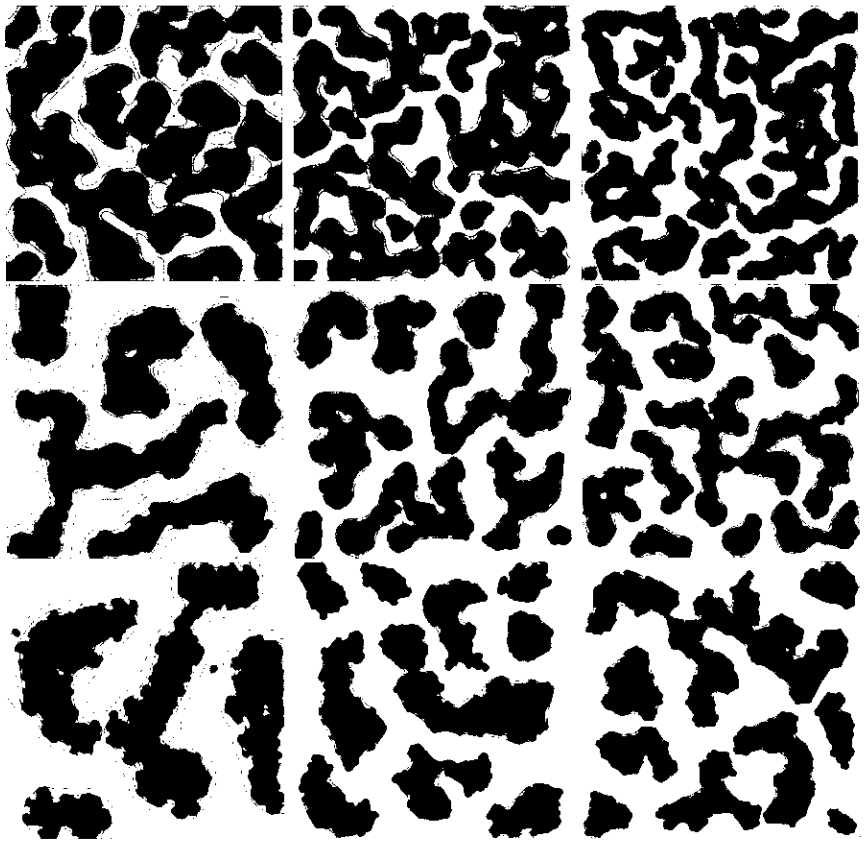

Figure 10: Across: Increasing Concentrations of MGP ($\gamma_v = .1, .5, .9$). Down:Increasing concentrations of BMP-2 ($\gamma_u = .1, .5, .9$). At 20000 MCS. There are 1350 cells in this simulation.

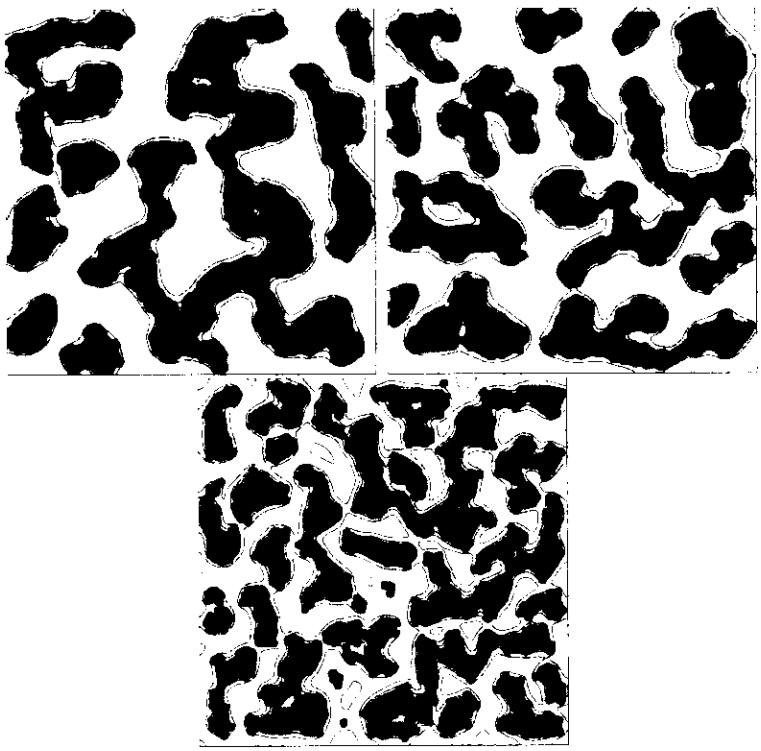

Figure 11: After 20000 MCS. The source term$S$ is 0,.3, and 3. $\gamma_v = \gamma_u = .5$. There are 1350 cells in this simulation.

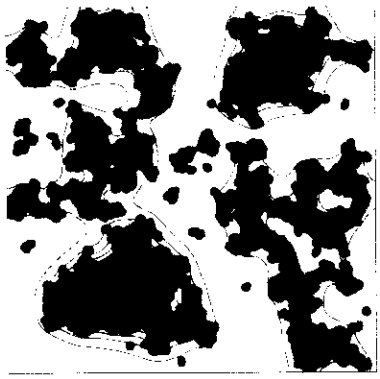

Figure 12: After 30000 MCS. $S = .6$, $\gamma_v = .1$, and $\gamma_u = .9$, 1350 is initial number of cells. Changing the production rates of the inhibitor and chemoattractant while still adding a source term does make the pattern form a mix of a spot and stripes.

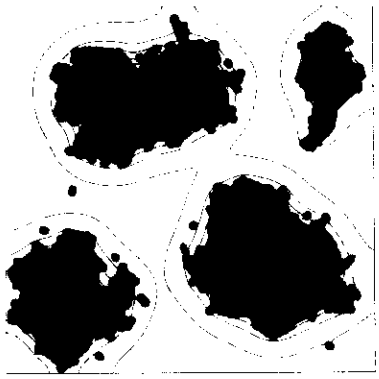

Figure 13: After 80000 MCS. $S = .6$, $\gamma_v = .1$, and $\gamma_u = .9$. Starting with 1350 cells and running for more MCS makes spots form.

4 Conclusions

The cellular Potts model can reproduce spots and stripes without the autocatalytic term and including cellular dynamics, making the model more biologically realistic. However, the model needs some modifications to completely reproduce the results, For instance, the spots are not formed by the addition of a source term, S. In Garfinkel et al.'s reaction-diffusion model, when they added the source term, they added it over a short period of time. For future work on this cellular Potts model, we would change how the source term is added so that it too is only added over a few Monte Carlo steps, instead of every Monte Carlo step. Then the added MGP would still effect the pattern formation, but would not overwhelm the system.

There are very few "Y-connections" in the simulations producing stripes. Perhaps altering some of the parameters, such as cell adhesion values, would make the cells interconnect more. Even though adding more cells to the simulation makes the stripes more connected, a truly labyrinthine pattern does not appear. In reaction-diffusion models, patterns can be altered by a saturation term [11]. As shown in Fig. 5, altering the saturation term changes the pattern from stripes to spots. Altering k further may also help increase the number of "Y-connections". Such modifications to explore how to make the stipes more labyrinthine are left for future work.

The cellular Potts model predictions are limited by the simulation size. As the size of the lattice increases, the time it takes to complete each Monte Carlo step increases significantly. It is also hard to run many Monte Carlo steps because of the extremely long time it takes. However, there are some encouraging aspects of the cellular Potts model. Once more cells were added to the system initially, the stripes interconnected more. Also, the cellular Potts model does show the formation of spots after several Monte Carlo steps. Further modifications to the parameters of increase "Y-connections", and changing how the source term is added on the model may predict the formation of more of the patterns.

5 Acknowledgements

I want to thank Roeland Merks and Stephen Teitel for all their help and advice throughout the process of writing this thesis. I also want to thank Roeland Merks for the use of his code that I modified to do the simulations.

References

[1] Tintut, Y., Alfonso, Z., Saini, T., Radcliff, K., Watson, K., Bostrom, K. & Demer, L. (2003) *Circulation* **108**, 2505-2510.

[2] Bostrom, K., Warson, K., Horn, S., Wortham, C., Herman, I., & Demer, L. (1993) *J. Clin. Invest.***91**, 1800-1809.

[3] Garfinkel, A., Tintut, Y., Petrasek, D., Bostrom, K., Demer, L.:Pattern formation by vascular mesenchymal cells. PNAS **101** (2004) 9247-9250.

[4] Garfinkel, A., Tintut, Y., Petrasek, D., Bostrom, K., Demer, L.:Supporting Text. PNAS http://www.pnas.org/cgi/content/full/0308436101/DC1.

[5] Merks, R., Newman, S., Glazier, J.:Cell Oriented Modeling of *in vitro* Capilary Development. ACRI (2004).

[6] Turing, A.:The Chemical Basis of Morphogenesis. (1952) *Philos. Trans. R. London* **237**, 37-72.

[7] Zebboudj, A. F., Imura, M., Bostom, K.:Matrix GLA protein, a regulatory protein for bone morphogenetic protein-2. *Journal of Biological Chemistry***277** (2002) 4388-4394.

[8] Savill, N., Hogeweg, P.:Modelling Morphogenesis: From Single Cells to Crawling Slugs. *J. theor. Biol.* (1997) **184**, 229-235.

[9] Glazier,J., Graner, F.:Simulation of the differential adhesion driven rearrangement of biological cells. *Physical Review E* (1992)**47** 2128-2154.

[10] Gilbert, S. :Developmental Biology. 4th Ed. Sinaur Associates, Inc. 1994.

[11] Gierer, A. Meinhardt, H. (1972) *Kybernetik* **12**, 30-39.

[12] Merks, R. Glazier, J.: A cell-centered approach to developmental biology. *Physica A* (2005).